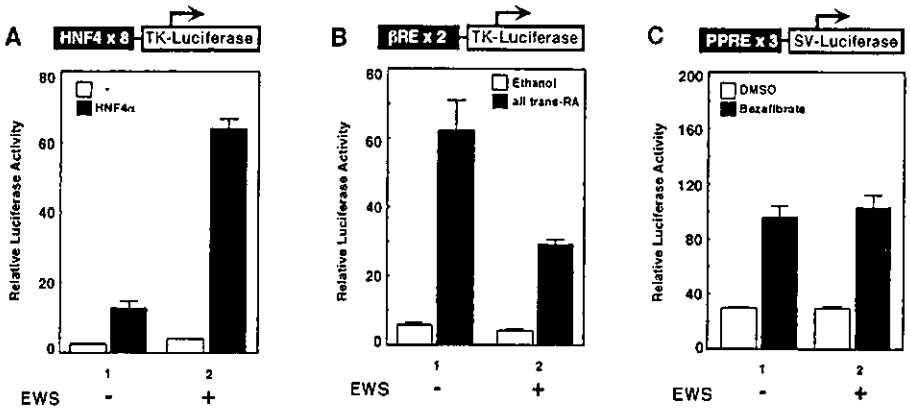

FIG. 3. **Selective enhancement of HNF4-mediated transactivation by EWS.** *A*, HEK293 cells were transiently transfected with 50 ng of pHNF4x8-tk-Luc reporter plasmid and absence (*open bars*) or presence (*filled bars*) of 25 ng of HNF4α and 100 ng of EWS expression plasmid. *B*, HEK293 cells were transfected with 100 ng of pβREx2-tk-Luc for retinoic acid receptor and 100 ng of EWS expression plasmid. After transfection, cells were treated with Phenol Red-free minimum Eagle's medium with 10% fetal bovine serum either alone (*open bars*) or with 1 μM all-*trans*-retinoic acid (*filled bars*). *C*, HEK293 cells were transfected with 10 ng of pPPREx3-sv-Luc for peroxisome proliferator-activated receptor α and 100 ng of EWS expression plasmid. After transfection, cells were incubated in the absence (*open bars*) or presence (*filled bars*) of 500 μM Bezafibrate. The results are the means ± S.E. of at least three independent experiments performed in duplicate. *DMSO*, Me_2SO.

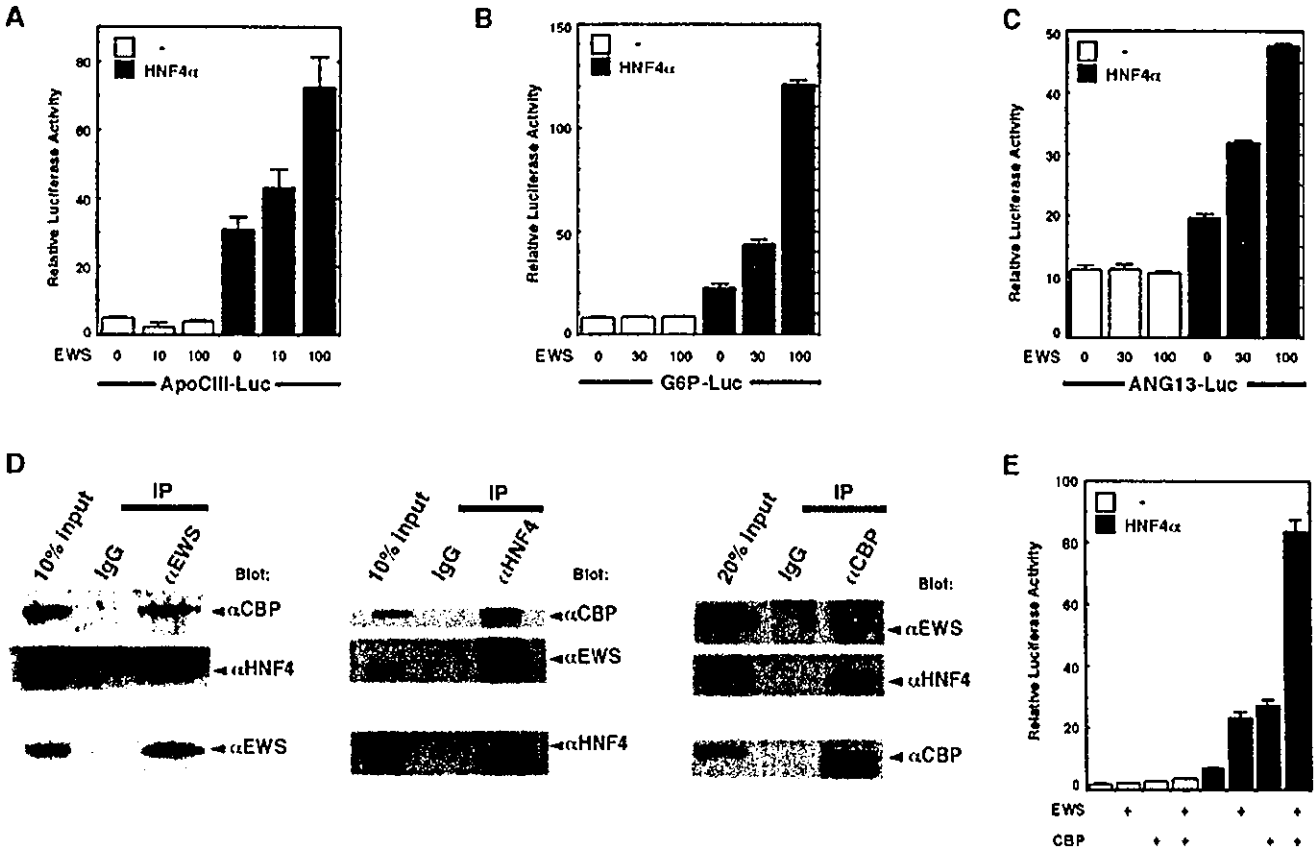

FIG. 4. **Formation of EWS, CBP, and HNF4 complex and cooperative enhancement of HNF4-dependent transactivation.** Enhancement of endogenous promoter sequences by EWS. HEK293 cells were transfected with 10 ng of ApoCIII-Luc (*A*), G6P-Luc (*B*), or 50 ng of angiotensinogen 13-Luc reporter plasmid (*C*), 25 ng of HNF4α expression plasmid, and the indicated amounts of EWS expression plasmid. These results represent the mean ± S.E. of at least three experiments. *D*, co-immunoprecipitation of endogenous CBP/HNF4, CBP/EWS, and EWS/HNF4 using anti-EWS, anti-HNF4, or anti-CBP antibodies. Nuclear extracts from HepG2 cells were immunoprecipitated with anti-EWS (α*EWS*; *left*), anti-HNF4 (α*HNF4*; *center*), and anti-CBP (αCBP; *right*) antibodies or normal rabbit IgG as a control and then were subjected to immunoblotting with anti-EWS, anti-CBP-(5614) or anti-HNF4α (C-19) antibodies. *E*, EWS and CBP cooperatively enhance HNF4-mediated transactivation. Cells were transfected with 50 ng of pHNF4x8-tk-Luc reporter plasmid, 25 ng of HNF4α expression plasmid, 100 ng of EWS expression plasmid, and 250 ng of CBP expression plasmid. This result is the means ± S.E. of at least three independent experiments performed in duplicate.

erase reporter plasmids containing each HNF4-targeted gene promoter. EWS enhanced ApoCIII (Fig. 4*A*), G6P (Fig. 4*B*), or angiotensinogen (Fig. 4*C*) reporters, which were activated by HNF4 in a dose-dependent manner. To confirm the interaction of HNF4, CBP, and EWS under more physiological conditions, endogenous EWS, HNF4, and CBP in HepG2 nuclear extracts were co-immunoprecipitated with anti-EWS, anti-HNF4, and anti-CBP antibodies, respectively. As shown in Fig. 4*D*, endogenous EWS, HNF4, and CBP could be efficiently co-immunoprecipitated with endogenous CBP/HNF4, CBP/EWS, and

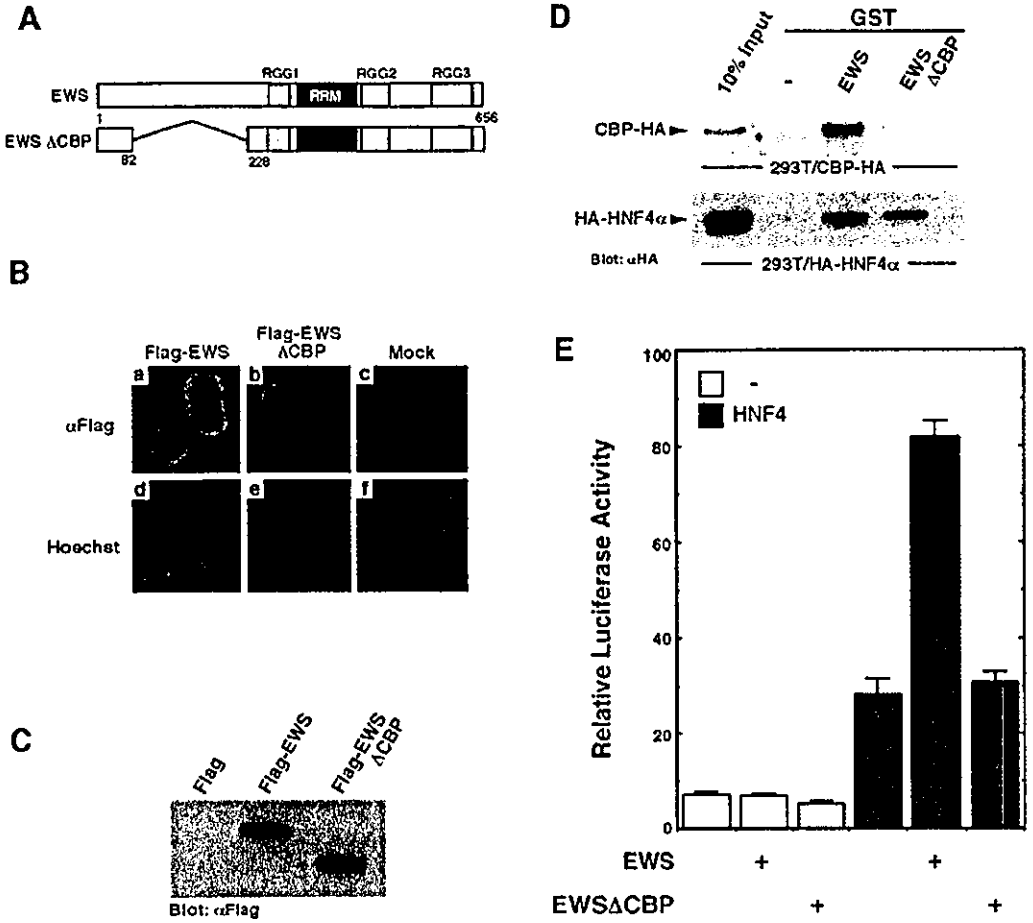

FIG. 5. **Requirement of CBP for EWS function.** *A*, schematic representation of EWSΔCBP, which lacks the amino acids 83–227 in EWS. *B*, subcellular localization of EWS and EWSΔCBP. HEK293T cells were transfected with FLAG-tagged EWS (*panels a* and *d*) and EWSΔCBP (*panels b* and *e*) expression plasmids or an empty plasmid (*panels c* and *f*) and were stained with anti-FLAG antibody (M2) (*panels a*, *b*, and *c*) or Hoechst (*panels d*, *e*, and *f*). *C*, Western blot analysis of FLAG-tagged EWS and EWSΔCBP. Cell extracts from HEK293 cells transfected with FLAG-tagged EWS or EWSΔCBP expression plasmid were immunoblotted with anti-FLAG antibody (M2). *D*, pull-down assays with EWS or EWSΔCBP fused to GST and extracts from HEK293T cells overexpressing HA-tagged CBP (*upper panel*) or HNF4α (*lower panel*). Western blot analyses were performed with an anti-HA antibody (12CA5). *E*, EWS but not EWSΔCBP enhances the HNF4-dependent transactivation. HEK293 cells were transfected with 50 ng of pHNF4x8-tk-Luc reporter plasmid, 25 ng of HNF4α, and 100 ng of EWS or EWSΔCBP expression plasmid followed by luciferase assay. This result is the means ± S.E. of at least three independent experiments performed in duplicate.

EWS/HNF4, respectively. To assess the regulatory effects of EWS and CBP on HNF4-mediated transactivation, we performed the reporter assay. Transfected HNF4 activity evaluated by co-transfection with an HNF4-tk-Luc reporter was further increased 3–4-fold by overexpression of EWS or CBP. When co-transfected together, both vectors induced reporter activity 13-fold in HNF4-transfected but not in non-transfected cells, suggesting that these transcription factors function cooperatively in HNF4-dependent transactivation (Fig. 4*E*).

Requirement of CBP for EWS Function—To determine whether the interaction with CBP is required for EWS-mediated activation, we constructed EWSΔCBP, which lacks the CBP-binding region (amino acids 83–227) (Fig. 5*A*). We first compared expression patterns of FLAG-tagged EWS or EWSΔCBP in transfected HEK293 cells by immunofluorescence and Western blot analyses with an anti-FLAG antibody. As shown Fig. 5, *B* and *C*, FLAG-tagged EWSΔCBP as well as EWS was localized in the nucleus, and these expression levels were nearly equal. We next tested the binding activity of EWSΔCBP with CBP or HNF4 by GST pull-down assays. As shown in Fig. 5*D*, EWSΔCBP lost the interaction with transfected HA-tagged CBP (*upper panel*) but still bound to HA-tagged HNF4α (*lower panel*). We then assessed the effect of EWSΔCBP on HNF4-mediated transactivation by transient transfection assay. In HEK293 cells, an HNF4-tk-Luc reporter was inactive because of little expression of endogenous HNF4 protein (Fig. 5*E*, *lanes 1–3*). The luciferase reporter was activated up to 3-fold by co-transfection with HNF4 (Fig. 5*E*, *lane 4*). The addition of EWS resulted in additional 2.5-fold activation (Fig. 5*E*, *lane 5*). However, in the presence of HNF4, co-transfection with EWSΔCBP did not activate the HNF4-dependent transactivation (Fig. 5*E*, *lane 6*). These results suggest that interaction with CBP is required for the activity of EWS on HNF4-dependent transactivation through the CBP-binding region.

DISCUSSION

EWS was originally identified as a fusion protein with Fli-1 in Ewing's sarcoma and was later found in several malignancies in which the NTD of EWS was fused to the DNA-binding domain of the ETS family such as ATF-1, WT-1, CHN, and C/EBP homologous protein (2). For all of the above malignancies, the EWS fusion proteins are thought to act as potent transcriptional activators in a manner that is dependent on the transcriptional activation domain in the NTD of EWS (22). However, the transcriptional function of native EWS is not very well understood. It has been shown that transcriptional

events are closely coupled with processing events *in vivo* (17, 18). The C-terminal domain of the largest subunit of Pol II plays a central role in this coupling by reversible phosphorylation during the transcription cycle. Once initiation of transcription begins, the hypophosphorylated form of C-terminal domain (Pol IIa) becomes hyperphosphorylated (Pol IIo) during the transition from the preinitiation complex to the elongation-processing complex, and this form of pol II is able to recruit mRNA processing factors (23). EWS was previously reported to interact with only Pol IIo as an adaptor molecule to recruit splicing factors in elongation stages (2).

In this study, we identified the interaction of EWS with CBP and with both of the preinitiation (Pol IIa) and the elongation (Pol IIo) forms of Pol II. CBP associates only with Pol IIa (24) (Fig. 2) and activates transcriptional initiation as a bridging/co-activating/chromatin-remodeling factor. These findings suggest that EWS may activate transcriptions in collaboration with CBP and basal transcription machinery including the preinitiation form (Pol IIa) of Pol II complex.

A previous study (25) showed the interaction of EWS with CBP/p300 and the activation of c-*fos*, *Xvent-2*, and *Erb2* promoters by EWS. Because EWS does not have any obvious DNA-binding domain, it has been described that EWS may be recruited to target promoters by protein-protein interaction with DNA-binding transcription factors and act as a co-activator. However, a target DNA-binding transcription factor has not yet been identified. We demonstrated that EWS selectively potentiates the DNA-binding HNF4 transcription factor-mediated transactivation (Fig. 3). As transient transfection analyses using the *ApoCIII*, *G6P*, and *angiotensinogen* promoters illustrated that these were activated by HNF4 in conjunction with EWS but not in the absence of HNF4, HNF4 is a high affinity site for the entry of EWS to the target promoters. On the other hand, EWS repressed RAR-mediated transcription (Fig. 3*B*) and did not associate with RAR under the conditions used in this assay (data not shown). This finding suggested that RAR is not a direct target molecule of EWS and that the repression by EWS artificially arises from squelching CBP, RNA polymerase II, TFIID, or other factors in the transcriptional complex for RAR.

We found that EWS interacted with CBP and HNF4 and played cooperatively with CBP to further reinforce the transactivation of HNF4 (Fig. 4). In addition, the co-activational activity of EWS was abolished by the deletion of the CBP-binding region of EWS (amino acids 83–227) (Fig. 5). In previous studies, Ohno *et al.* (26) and Lessnick *et al.* (27) demonstrate that the transcriptional activity of EWS is included in amino acids 83–265 when fused to the DNA-binding domain of GAL4 or *Fli-1*. These findings reveal that the co-activator function of CBP mediates the transactivation ability of EWS or EWS fusion proteins through the NTD.

Although we demonstrated that EWS interacts with CBP and the preinitiation form of Pol II and enhances HNF4-mediated transcription in a manner dependent on the co-activator function of CBP, additional EWS functions were suggested by other studies. For example, EWS contains motifs like RNA-binding proteins and actually binds to RNA *in vitro* (28), the elongation-mRNA processing form of pol II (Pol IIo) (Fig. 2) (9, 10), and the splicing factors (7–9). Furthermore, it has been shown that EWS-Fli-1 can antagonize the splicing of model mRNA constructs in cells (9, 10). In this point, PPARγ co-activator-1, which has also been reported as an HNF4 co-activator (29), can function as both transcriptional co-activator and splicing regulator (30). Thus, our present findings provide the possibility that a variety of HNF4-dependent physiological functions including fatty acid metabolism, gluconeogenesis, and blood pressure control may be exerted efficiently as results of coupling of between transcription and mRNA processing by EWS and/or PPARγ co-activator-1.

Because EWS is a ubiquitously expressed factor (31) as compared with the limited expression profile of PPARγ co-activator-1 in the brown fat, kidney, heart, and brain under the normal conditions (32), it is likely that EWS participates in various biological events through other nuclear receptors or CBP-directed DNA-binding transcription factors. In contrast, we confirmed that a EWS fusion gene, *EWS-Fli-1*, lost the activity as a co-activator by a minimal reporter gene system using HNF4 recognition site (data not shown). It is expected that impaired (lost or acquired) biological systems of native EWS caused by a gene fusion event may be related to the tumorigenesis. Therefore, further analysis regarding the native EWS function will be helpful to understand the physiological significance of EWS in addition to the mechanisms of transformation by EWS fusion proteins.

Acknowledgment—We thank the Fukamizu laboratory members for helpful discussion and encouragement.

REFERENCES

1. Delattre, O., Zucman, J., Plougastel, B., Desmaze, C., Melot, T., Peter, M., Kovar, H., Joubert, I., de Jong, P., Rouleau, G. *et al.* (1992) *Nature* **359**, 162–165
2. Arvand, A. & Denny, C. T. (2001) *Oncogene* **20**, 5747–5754
3. Burd, C. G. & Dreyfuss, G. (1994) *Science* **265**, 615–621
4. Bentley, D. (1999) *Curr. Opin. Cell Biol.* **11**, 347–351
5. Bertolotti, A., Melot, T., Acker, J., Vigneron, M., Delattre, O. & Tora, L. (1998) *Mol. Cell. Biol.* **18**, 1489–1497
6. Petermann, R., Mossier, B. M., Aryee, D. N., Khazak, V., Golemis, E. A. & Kovar, H. (1998) *Oncogene* **17**, 603–610
7. Zhang, D., Paley, A. J. & Childs, G. (1998) *J. Biol. Chem.* **273**, 18086–18091
8. Knoop, L. L. & Baker, S. J. (2000) *J. Biol. Chem.* **275**, 24865–24871
9. Yang, L., Chansky, H. A. & Hickstein, D. D. (2000) *J. Biol. Chem.* **275**, 37612–37618
10. Chansky, H. A., Hu, M., Hickstein, D. D. & Yang, L. (2001) *Cancer Res.* **61**, 3586–3590
11. Goodman, R. H. & Smolik, S. (2000) *Genes Dev.* **14**, 1553–1577
12. Vo, N. & Goodman, R. H. (2001) *J. Biol. Chem.* **276**, 13505–13508
13. Yoshida, E., Aratani, S., Itou, H., Miyagishi, M., Takiguchi, M., Osumu, T., Murakami, K. & Fukamizu, A. (1997) *Biochem. Biophys. Res. Commun.* **241**, 664–669
14. Chakravarti, D., LaMorte, V. J., Nelson, M. C., Nakajima, T., Schulman, I. G., Juguilon, H., Montminy, M. & Evans, R. M. (1996) *Nature* **383**, 99–103
15. Yanai, K., Hirota, K., Taniguchi-Yanai, K., Shigematsu, Y., Shimamoto, Y., Saito, T., Chowdhury, S., Takiguchi, M., Arakawa, M., Nibu, Y., Sugiyama, F., Yagami, K. & Fukamizu, A. (1999) *J. Biol. Chem.* **274**, 34605–34612
16. Miyagishi, M., Fujii, R., Hatta, M., Yoshida, E., Araya, N., Nagafuchi, A., Ishihara, S., Nakajima, T. & Fukamizu, A. (2000) *J. Biol. Chem.* **275**, 35170–35175
17. Payne, J. M., Laybourn, P. J. & Dahmus, M. E. (1989) *J. Biol. Chem.* **264**, 19621–19629
18. Dahmus, M. E. (1995) *Biochim. Biophys. Acta* **1261**, 171–182
19. Mietus-Snyder, M., Sladek, F. M., Ginsburg, G. S., Kuo, C. F., Ladias, J. A., Darnell, J. E., Jr. & Karathanasis, S. K. (1992) *Mol. Cell. Biol.* **12**, 1708–1718
20. Rajas, F., Gautier, A., Bady, I., Montano, S. & Mithieux, G. (2002) *J. Biol. Chem.* **277**, 15736–15744
21. Li, J., Ning, G. & Duncan, S. A. (2000) *Genes Dev.* **14**, 464–474
22. Kim, J. & Pelletier, J. (1999) *Physiol. Genomics* **1**, 127–138
23. Corden, J. L. & Patturajan, M. (1997) *Trends Biochem. Sci.* **22**, 413–416
24. von Mikecz, A., Zhang, S., Montminy, M., Tan, E. M. & Hemmerich, P. (2000) *J. Cell Biol.* **150**, 265–273
25. Rossow, K. L. & Janknecht, R. (2001) *Cancer Res.* **61**, 2690–2695
26. Rao, V. N., Ohno, T., Prasad, D. D., Bhattacharya, G. & Reddy, E. S. (1993) *Oncogene* **8**, 2167–2173
27. Lessnick, S. L., Braun, B. S., Denny, C. T. & May, W. A. (1995) *Oncogene* **10**, 423–431
28. Ohno, T., Ouchida, M., Lee, L., Gatalica, Z., Rao, V. N. & Reddy, E. S. (1994) *Oncogene* **9**, 3087–3097
29. Yoon, J. C., Puigserver, P., Chen, G., Donovan, J., Wu, Z., Rhee, J., Adelmant, G., Stafford, J., Kahn, C. R., Granner, D. K., Newgard, C. B. & Spiegelman, B. M. (2001) *Nature* **413**, 131–138
30. Monsalve, M., Wu, Z., Adelmant, G., Puigserver, P., Fan, M. & Spiegelman, B. M. (2000) *Mol. Cell* **6**, 307–316
31. Alliegro, M. C. & Alliegro, M. A. (1996) *Dev. Biol.* **174**, 288–297
32. Puigserver, P., Wu, Z., Park, C. W., Graves, R., Wright, M. & Spiegelman, B. M. (1998) *Cell* **92**, 829–839

Journal of Pediatric Hematology/Oncology, Vol. 25, No. 9, September 2003

Original Article

Gene and Protein Expression Profiling During Differentiation of Neuroblastoma Cells Triggered by 13-cis Retinoic Acid

Yuki Yuza, MD, Miyuki Agawa, Masaharu Matsuzaki, PhD, Hisashi Yamada, MD, PhD, and Mitsuyoshi Urashima, MD, MPH, PhD

Purpose: The precise changes in RNA and protein expression that accompany neuroblastoma differentiation remain unknown. The authors used microarray technologies to screen molecules associated with the differentiation of neuroblastoma (NB) cells induced by 13-cis retinoic acid.

Methods: The authors quantified the expression of 2,061 RNA transcripts related to oncogenesis and of 380 proteins expressed in SK-N-SH and CHP-134 NB cell lines in the presence or absence of 13-cis retinoic acid.

Results: Hierarchical clustering captured gene expression altered during neuroblastoma differentiation induced by 13-cis retinoic acid. Several genes were further abstracted based on *P* values below 0.0017 or protein chips observed in both NB cell lines. The altered expressions of gene products revealed by both DNA and protein chips were in agreement. The expressions of N-*myc*, cyclin D3, and Wnt10B were downregulated, whereas those of retinoblastoma (RB) and related genes (p107, RB2/p130, p300/CBP, E2F-1, DP-1) as well as others were upregulated.

Conclusions: These results suggest that microarray technology can screen for genes that are important in neuroblastoma differentiation.

Key Words: cis-retinoic acid, differentiation, isotretinoin, neuroblastoma, oligodeoxyribonucleotide array sequence analysis, protein array assay, retinoblastoma protein

Neuroblastoma (NB) originating from the neural crest is one of the most common solid tumors arising in young children. The clinical course of patients with NB varies from spontaneous regression to a very poor prognosis.[1] Despite the use of high-dose chemotherapies with hematopoietic stem cell support, the prognosis of advanced NB, especially with N-*myc* gene amplification, remains very poor.[2,3] Although new treatment strategies such as 131-I-metaiodobenzylguanidine (131-I-MIBG) and immunotherapy have shown potential to improve the outcome,[4–6] further advances in drug therapy are desirable to prevent relapse and to improve the prognosis of patients with advanced NB.

The vitamin A derivative 13-cis retinoic acid (isotretinoin) has improved the 3-year event-free survival of advanced NB from 29 ± 5% to 46 ± 6%,[7] although another study with different doses and schedules failed to show similar efficacy.[8] Isotretinoin induces the growth arrest and differentiation of NB cell lines in vitro.[9,10] Thus, to screen molecules linked to NB cell differentiation triggered by 13-cis retinoic acid might identify new drugs that could treat NB, just as imatinib mesylate, a selective inhibitor of BCR-ABL tyrosine kinase, can treat chronic myeloblastic leukemia.[11]

Several studies have examined the roles of specific gene products in neuronal differentiation, such as the HMGI(Y) gene,[12] multidrug resistance-associated protein (MRP1),[13] galanin, and the galanin receptor.[14] However, changes in the expression of other genes must be associated with NB differentiation induced by 13-cis retinoic acid. Microarray technology was developed for the large-scale analysis of RNA and protein expression. These technologies allow the rapid, simple, and parallel detection of thousands of RNA transcripts in a single experiment.

We therefore used DNA and protein chips to screen for genes associated with the differentiation of two NB cell lines induced by 13-cis retinoic acid. Both types of chips revealed the concordant altered expression of several genes, indicating that microarray technologies represent a powerful first-line screening tool.

Submitted for publication November 5, 2002; accepted May 28, 2003.

From the Department of Pediatrics (Y.Y., M.U.), Department of Oncology, Institute of DNA Medicine (M.A.), Department of Molecular Genetics, Institute of DNA Medicine (H.Y.), and Division of Clinical Research and Development (M.U.), Jikei University School of Medicine, Tokyo, Japan; and BD Biosciences Clontech, Tokyo, Japan (M.M.).

Supported by Grant in Aid for Scientific Research.

Address correspondence and reprint requests to Mitsuyoshi Urashima, MD, PhD, MPH, Jikei University School of Medicine, 3-25-8, Nishi-shimbashi, Minato-ku, Tokyo 105-8461, Japan. E-mail: urashima@jikei.ac.jp.

METHODS

Cell culture

Human SK-N-SH NB cells[15] and CHP-134 NB cells[16] obtained from Riken GenBank (Riken, Saitama Prefecture, Japan) were cultured in RPMI 1640 medium (Sigma Chemical Co., St. Louis, MO) containing 10% fetal calf serum. The cells were maintained at 37°C under 5% CO_2/95% humidified air. Cells were seeded at an initial density of 10^4 cells/cm^2 in 75-cm^2 culture dishes (Corning, Corning, NY) until they reached 60% confluence. At that time, 13-cis retinoic acid (Sigma) was added to a final concentration of 8 mmol/L from a stock of 33 mmol/L in ethanol,[17,18] and the cells were collected 48 hours later for DNA chip analysis and after 72 hours for protein chip analysis without using trypsin. An equivalent amount of ethanol was added to control cells. All cells were sedimented by centrifugation and the pellets were washed three times with phosphate-buffered saline and then placed on ice.

RNA extraction and DNA chip assays

Total RNA (approximately 2 μg) was immediately extracted from the pellets after 48 hours of culture using the RNeasy Kit (Qiagen K.K., Tokyo, Japan). Complementary RNA was generated from the total RNA and hybridized to human HC-G110 oligonucleotide probe arrays (Affymetrix, Santa Clara, CA) according to a standard protocol[19] that was specifically designed for oncogenesis. Arrays were subsequently scanned with phycoerythrin-conjugated streptavidin and biotinylated antibody against streptavidin and scanned to semi-quantify gene expression. All cell culture assays and the DNA chip procedure were repeated three times independently.

Protein chip

After 72 hours of culture, proteins were extracted from cell pellets by a single freeze/thaw cycle followed by resuspension in extraction labeling buffer containing nondenaturing detergents to maintain protein solubility and to emulsify membrane-bound proteins. Protein from each sample (10 μg) was labeled with green (Cy3) and red (Cy5) fluorescent dyes. Following a simple desalting step to remove unbound dye, the labeled proteins were incubated with each of the 380 antibody microarrays duplicated by each gene (BD Clontech Ab Microarray 380 [www.bdbiosciences.com/clontech], BD Biosciences Clontech, Tokyo, Japan).

Statistics

We analyzed RNA expression profiles as follows. Raw data from cells in the presence ($n = 3 \times 2$ cell lines $= 6$) or absence ($n = 3 \times 2$ cell lines $= 6$) of 13-cis retinoic acid were compared using a paired t test. Genes with a P value of 0.1 or more were deleted. This reduced the number of candidate oligo probes involved in NB differentiation from 2,061 to 825. Spotfire Decision Site 7.0 for functional genomics (Spotfire, Somerville, MA) was used to perform hierarchical clustering and to visualize datasets. Hierarchical clustering was determined following the log2 transformation of all raw data and normalization with z-scores for each gene. From these results, differences in raw expression values were further compared between the presence and absence of 13-cis retinoic acid using the t test, and statistical significance was established at $P < 0.017$. This value was obtained as follows—0.05/the square root of the number of genes in the analysis—to reduce type I errors. In the protein chip analysis, the ratio of Cy3 to Cy5 was calculated for each gene from all samples. The internally normalized ratio (INR) was then calculated as the ratio of the sample in the presence of retinoic acid divided by that in the absence.

RESULTS

Morphologic differentiation, defined as the elongation of neurites, was confirmed under phase-contrast microscopy in both SK-N-SH cells and CHP-134 cells after 48 hours in the presence of 13-cis retinoic acid.[9,10] Mean of the raw data obtained from three independent experiments were compared for each gene by t tests comparing the presence and absence of 13-cis retinoic acid. We applied hierarchical clustering of 825 genes filtered with P value below 0.1 in the t tests to detect specific changes in NB differentiation (Fig. 1). The dendrogram of hierarchical clustering indicated that differences between the absence and presence of 13-cis retinoic acid were less than the differences between cell lines. We then selected gene clusters with obviously altered RNA expression (upregulation or downregulation) between the presence and absence of 13-cis retinoic acid in both cell lines. The expression of various genes was downregulated in the presence of 13-cis retinoic acid (Fig. 2). In particular, expressions of N-*myc* and Wnt10B were significantly reduced, which were confirmed by both gene and protein chip. Decreased expression of cyclin D3 was confirmed only by protein chip. In contrast, the expression of other genes was upregulated in the presence of retinoic acid (Fig. 3). The expressions of N-*ras*, tumor necrosis factor receptor-associated death domain protein (TRADD), BMX, human epidermal growth factor receptor 2 (HER2), and retinoblastoma susceptible gene 1 (RB1) were significantly increased in both cell lines. In addition, the RNA expressions of RB2/p130, E2F-1, TRADD, BMX, Wilms tumor associated protein 1 (WT1), BCL2, transforming growth factor (TGF)-beta, cadherin, p300, casein kinase II alpha subunit, HER2, heat shock protein 90, and DP-1 were increased consistently with the findings using the protein chip.

DISCUSSION

Microarray technology has become a conventional tool with which to explore factors associated with clinical results

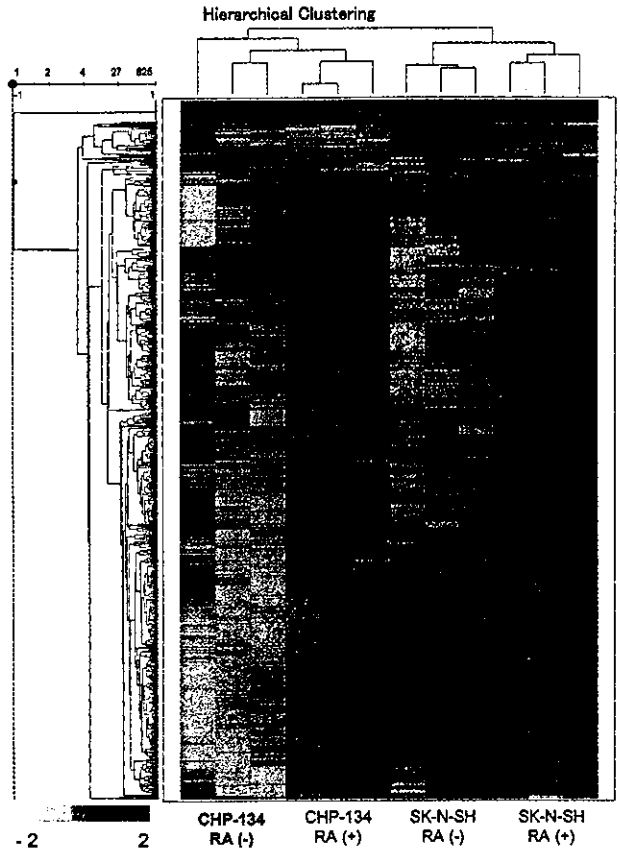

FIGURE 1. Hierarchical clustering of changes of RNA expression in both SK-N-SH and CHP-134 cells cultured for 48 hours with or without 13-cis retinoic acid. Relative red intensity is pseudo-colored such that red and green indicate high (z-scores $\geq$ 2) and low expression (z-scores $\leq$ – 2), respectively.

or biologic phenomena. Although the *t* test may be used conservatively to avoid type I error due to high volume variables, hierarchical clustering is often applied to the data analysis of microarrays. However, the results obtained by hierarchical clustering may include significant background noise. Moreover, protein chips may have the advantage in identifying genes for ubiquitous proteins compared with DNA chips, because protein levels in the cells are regulated not only by RNA expression levels but also by degradative pathways. Therefore, we used protein chips to validate the expression of several of the genes that were altered in the RNA expression analyses. The direction of expression of genes covered by both DNA and protein chips was concordant between them, although degrees of amplification did not always match.

The present study confirmed that retinoic acid decreases N-*myc* RNA expression levels.[20,21] As described,[22] the N-*myc* gene was not amplified in SK-N-SH cells. In contrast, N-*myc* was amplified 14-fold in CHP-134 cells, but the level of N-*myc* gene amplification was not altered at 24 and 48 hours of culture after exposure to 13-cis retinoic acid (data not shown).

Some genes that were significantly different within expression patterns in this study are in fact associated with neuronal differentiation. TRADD is involved in the neurotrophin receptor (p75NTR)-mediated anti-apoptotic activity of nerve growth factor in breast cancer cells,[23] WNT10B mRNA expression is downregulated by all-*trans* retinoic acid in NT2 cells with the potential of self-renewal and neuronal differentiation,[24] and insulin-like growth factor I induces cell proliferation and differentiation of NB cells through insulin receptor substrate-1 (IRS-1).[25] In some cell types, particularly muscle cells, ras inhibits differentiation, whereas in others, such as neuronal, adipocytic, or myeloid cells, ras induces differentiation, sometimes accompanied by growth arrest.[26] Other genes not known to be associated with NB differentiation include HER2, an epidermal growth factor receptor that is an essential mediator of cell proliferation and differentiation in the developing embryo and in some adult tissues. The activation of such genes is associated with the development and severity of many cancers.[27] The stage-specific expression of BMX is critical for the differentiation of myeloid cells,[28] and RIP is an important factor that controls keratinocyte and myogenic differentiation.[29,30]

The simultaneous alteration of functionally related genes in microarrays may be another way of screening for differentiation factors. All members of the RB family (RB1/p110, p107 and RB2/p130) share similar structures and functions and coordinate with E2F and DP-1 to modify cell cycle progression from the G1 to the S phase.[31] In this study, increased expression of RB1/p110 was confirmed by both

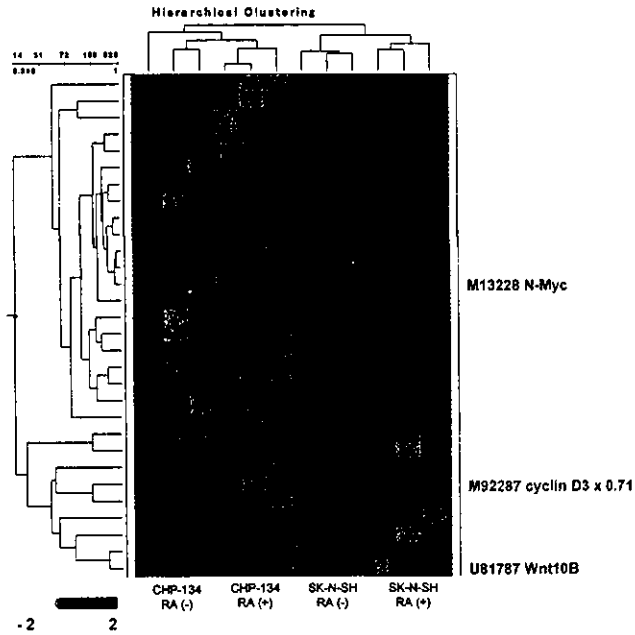

FIGURE 2. Cluster with downregulation of gene expression profiling triggered by 13-cis retinoic acid. Gene names in red mean that statistical difference was confirmed by both gene and protein chip. Gene names in blue mean that statistical differences were confirmed only by protein chip.

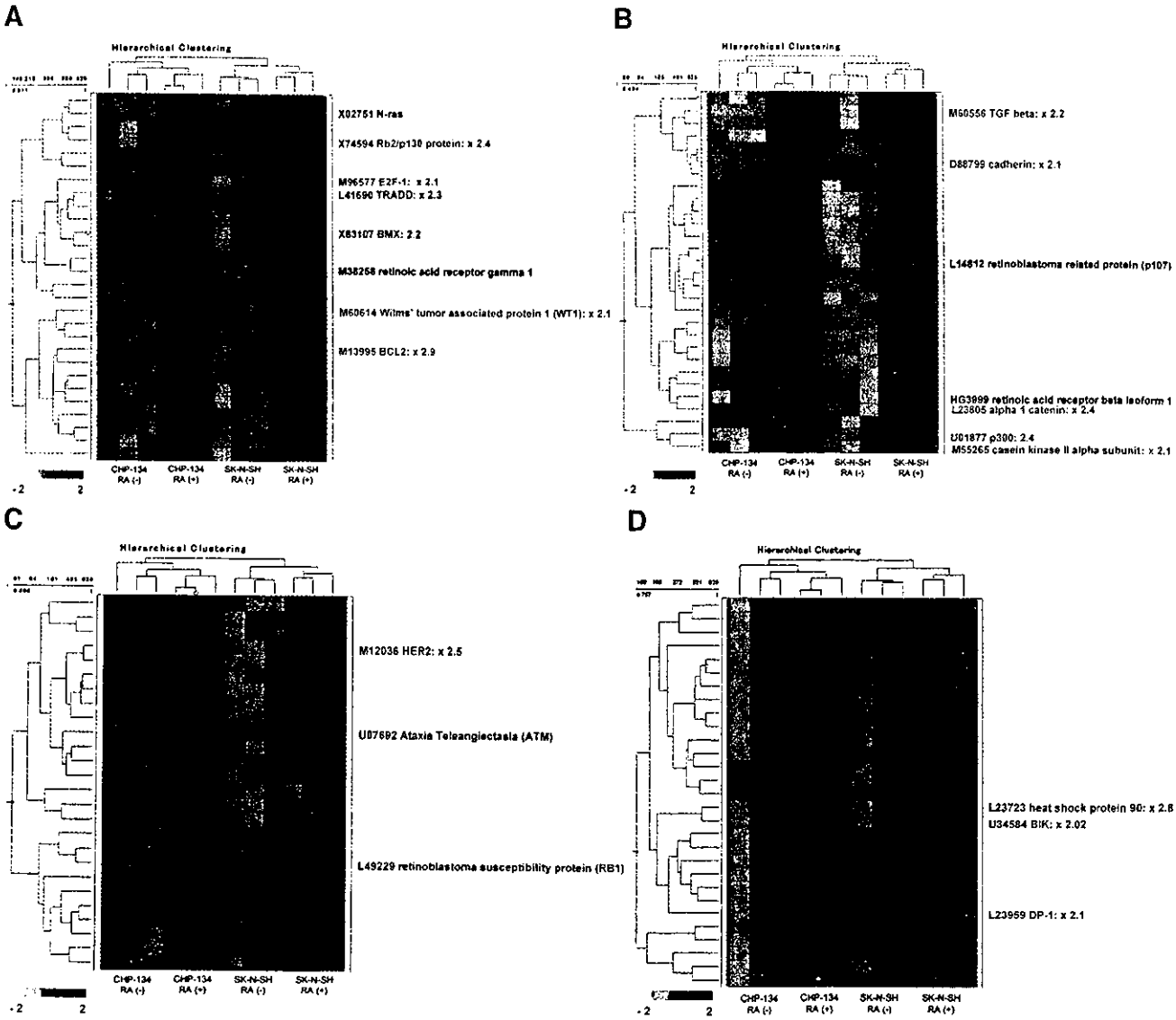

FIGURE 3. Clusters (**A–D**) with upregulation of gene expression profiling triggered by 13-cis retinoic acid. Gene names in red mean that statistical difference was confirmed by both gene and protein chip. Gene names in blue mean that statistical differences were confirmed only by protein chip. Gene names in black mean that statistical difference was not confirmed by either gene or protein chip.

gene and protein chip and increased expressions of RB2/p130, E2F and DP-1 were confirmed only by protein chip, although statistical changes in the expression of p107 were not confirmed by either gene or protein chip. Alterations in RNA levels of any gene may reflect either real differences in transcription or fluctuations in experimental conditions. However, these genes functionally associate with each other; the RB family induces G1 growth arrest by controlling the transcription factors E2F/DP-1 and p300/CBP,[32] whereas cyclin D3, a suppressor of RB function, was downregulated in this study.

Further, others have suggested that these molecules may significantly contribute to NB differentiation. Kranenburg et al discovered that neuronal differentiation can be induced by $p27^{KIP1}$ and RB overexpression.[33] The overexpression of RB1 induces neuronal differentiation that coordinates with nuclear restricted protein/brain.[34] In a murine NB model, RB2/p130 is highly upregulated during the middle to late stages of NB cell differentiation induced by DMSO.[35] RB2/p130 ectopic gene expression in NB cells induces a more differentiated NB phenotype.[36] Transfection of each member of the RB family (RB1, p107, and RB/p130) can induce neural differentiation and inhibit ^{3}H-thymidine incorporation.[37] In addition, increased expression of TGF-beta may activate RB family proteins through dephosphorylation.[38]

The altered expression of some other genes (BCL2, WT1, cadherin, alpha catenin, heat shock protein [HSP] 90, BIK, casein kinase II) captured in hierarchical clustering but not statistically different was detected using the protein

chips. Expression of the BCL2 proto-oncogene correlates with the differentiation characteristics of NB cell lines,[39] and WT1 expression in retinoblastoma may reflect the potential of these tumors to initiate the early steps of neuronal differentiation.[40] The expression of both N- and R-cadherin is related to optic nerve differentiation.[41] Catenin expression may be modulated by a variety of growth factors,[42] HSP90 can protect NB cells against apoptosis,[43] and casein kinase II promotes the phosphorylation of microtubule-associated protein, which contributes to the cytoskeletal scaffolding of growing neurites.[44,45] Retinoic acid receptors (RAR) beta and gamma were both upregulated in the present study.

Ferrati et al found that the induction of both RAR beta and RAR gamma controls the cell fate of apoptosis or differentiation.[46] In this study, since RAR beta and gamma were not available in protein chip, we could not confirm changes in expression of RAR beta and gamma.

In conclusion, the findings of the present study suggest that microarray technology can screen for genes that are important in neuroblastoma differentiation.

Acknowledgment: The authors thank Professor Yoshikatsu Eto, Chairman, Department of Pediatrics at Jikei University School of Medicine, for critical reading of this article.

REFERENCES

1. Nishihira H, Toyoda Y, Tanaka Y, et al. Natural course of neuroblastoma detected by mass screening: a 5-year prospective study at a single institution. *J Clin Oncol.* 2000;18:3012–3017.
2. Fulda S, Lutz W, Schwab M, et al. MycN sensitizes neuroblastoma cells for drug-triggered apoptosis. *Med Pediatr Oncol.* 2000;35:582–584.
3. Cotterill SJ, Pearson AD, Pritchard J, et al. Clinical prognostic factors in 1277 patients with neuroblastoma: results of the European Neuroblastoma Study Group Survey 1982–1992. *Eur J Cancer.* 2000;36:901–908.
4. Garaventa A, Bellagamba O, Lo Piccolo MS, et al. 131 I-metaiodobenzylguanidine (131 I-MIBG) therapy for residual neuroblastoma: a mono-institutional experience with 43 patients. *Br J Cancer.* 1999;81:1378–1384.
5. Mastrangelo S, Tornesello A, Diociaiuti L, et al. Treatment of advanced neuroblastoma: feasibility and therapeutic potential of a novel approach combining 131-I-MIBG and multiple drug chemotherapy. *Br J Cancer.* 2001;84:460–464.
6. Pession A, Prete A, Locatelli F, et al. Immunotherapy with low-dose recombinant interleukin 2 after high-dose chemotherapy and autologous stem cell transplantation in neuroblastoma. *Br J Cancer.* 1998;78:528–533.
7. Matthay KK, Villablanca JG, Seeger RC, et al. Treatment of high-risk neuroblastoma with intensive chemotherapy, radiotherapy, autologous bone marrow transplantation, and 13-Cis retinoic acid. *N Engl J Med.* 1999;341:1165–1173.
8. Kohler JA, Imeson J, Ellershaw C, et al. A randomized trial of 13-Cis retinoic acid in children with advanced neuroblastoma after high-dose therapy. *Br J Cancer.* 2000;83:1124–1127.
9. Sidell N, Altman A, Haussler MR, et al. Effects of retinoic acid (RA) on the growth and phenotypic expression of several human neuroblastoma cell lines. *Exp Cell Res.* 1983;148:21–30.
10. Thiele CJ, Reynolds CP, Israel MA. Decreased expression of N-myc precedes retinoic acid – induced morphological differentiation of human neuroblastoma. *Nature.* 1985;313:404–406.
11. Kantarjian H, Sawyers C, Hochhaus A, et al. Hematologic and cytogenetic responses to imatinib mesylate in chronic myelogenous leukemia. *N Engl J Med.* 2002;346:645–652.
12. Giannini G, Kim CJ, Marcotullio LD, et al. Expression of the HMGI(Y) gene products in human neuroblastic tumours correlates with differentiation status. *Br J Cancer.* 2000;83:1503–1509.
13. Peaston AE, Gardaneh M, Franco AV, et al. MRP1 gene expression level regulates the death and differentiation response of neuroblastoma cells. *Br J Cancer.* 2001;85:1564–1571.
14. Perel Y, Amrein L, Dobremez E, et al. Galanin and galanin receptor expression neuroblastic tumours: correlation with their differentiation status. *Br J Cancer.* 2002;86:117–122.
15. Biedler JL, Helson L, Spengler BA. Morphology and growth, tumorigenicity, and cytogenetics of human neuroblastoma cells in continuous coculture. *Cancer Res.* 1973;33:2643–2652.
16. Schlesinger HR, Gerson JM, Moorhead PS, et al. Establishment and characterization of human neuroblastoma cell lines. *Cancer Res.* 1976;36:3094–3100.
17. Khan AA, Villablanca JG. Pharmacokinetic studies of 13-Cis retinoic acid in pediatric patients with neuroblastoma following bone marrow transplantation. *Cancer Chemother Pharmacol.* 1996;39:34–41.
18. Villablanca JG, Khan AA, Avramis VI, et al. Phase I trial of 13-Cis retinoic acid in children with neuroblastoma following bone marrow transplantation. *J Clin Oncol.* 1995;13:894–901.
19. Golub TR, Slonim DK, Tamayo P, et al. Molecular classification of cancer: class discovery and class prediction by gene expression monitoring. *Science.* 1999; 286:531–537.
20. Nakamura M, Matsuo T, Stauffer J, et al. Retinoic acid decreases targeting of p27 for degradation via an N-myc-dependent decrease in p27 phosphorylation and an N-myc-independent decrease in Skp2. *Cell Death Differ.* 2003;10:230–239.
21. Knoepfler PS, Cheng PF, Eisenman RN. N-myc is essential during neurogenesis for the rapid expansion of progenitor cell populations and the inhibition of neuronal differentiation. *Genes Dev.* 2002;16:2699–2712.
22. Sadee W, Yu VC, Richards ML, et al. Expression of neurotransmitter receptors and myc protooncogenes in subclones of a human neuroblastoma cell line. *Cancer Res.* 1987;47:5207–5212.
23. El Yazidi- Belkoura I, Adriaenssens E, Dolle L, et al. Tumor necrosis factor receptor-associated death domain protein (TRADD) is involved in the neurotrophin receptor (p75NTR)-mediated anti-apoptotic activity of nerve growth factor in breast cancer cells. *J Biol Chem.* 2003;Feb:25.
24. Kirikoshi H, Katoh M. Expression and regulation of WNT10B in human cancer: up-regulation of WNT10B in MCF-7 cells by beta-estradiol and down-regulation of WNT10B in NT2 cells by retinoic acid. *Int J Mol Med.* 2002;10: 507–511.
25. Kurihara S, Hakuno F, Takahashi S. Insulin-like growth factor-I-dependent signal transduction pathways leading to the induction of cell growth and differentiation of human neuroblastoma cell line SH-SY5Y: the roles of MAP kinase pathway and PI 3-kinase pathway. *Endocrin J.* 2000;47:739–751.
26. Crespo P, Leon J. Ras proteins in the control of the cell cycle and cell differentiation. *Cell Mol Life Sci.* 2000;57:1613–1636.
27. Cho HS, Mason K, Ramyar KX, et al. Structure of the extracellular region of HER2 alone and in complex with the Herceptin Fab. *Nature.* 2003;421:756–760.
28. Ekman N, Arighi E, Rajantie I, et al. The Bmx tyrosine kinase is activated by IL-3 and G-CSF in a PI-3K dependent manner. *Oncogene.* 2000;19:4151–4158.
29. Holland P, Willis C, Kanaly S, et al. RIP4 is an ankyrin repeat-containing kinase essential for keratinocyte differentiation. *Curr Biol.* 2002;12:1424–1428.
30. Munz B, Hildt E, Springer ML, et al. RIP2, a checkpoint in myogenic differentiation. *Mol Cell Biol.* 2002;22:5879–5886.
31. Weinberg R. The retinoblastoma protein and cell cycle control. *Cell.* 1995;81: 322–330.
32. Morris L, Allen KE, La Thangue NB. Regulation of E2F transcription by cyclin E-Cdk2 kinase mediated through p300/CBP co-activators. *Nat Cell Biol.* 2000; 2:232–239.
33. Kranenburg O, Scharnhorst V, Van der Eb AJ, et al. Inhibition of cyclin-dependent kinase activity triggers neuronal differentiation of mouse neuroblastoma cells. *J Cell Biol.* 1995;131:227–234.
34. Kim Ta. Lim J, Ota S, et al. NRP/B, a novel nuclear matrix protein, associates with p110(RB) and is involved in neuronal differentiation. *J Cell Biol.* 1998; 141:553–566.
35. Raschella G, Tanno B, Bonetto F, et al. The RB-related gene RB2/p130 in neuroblastoma differentiation and in B-myb promoter down-regulation. *Cell Death Diff.* 1998;5:401–407.
36. Jori FP, GAlderishi U, Piegari E, et al. RB2/p130 ectopic gene expression in neuroblastoma stem cells: evidence of cell-fate restriction and induction of differentiation. *Biochem J.* 2001;360:569–577.
37. Tanno B, Bonetto F, Negroni A, et al. Retinoblastoma family proteins include differentiation and regulate B-myb expression in neuroblastoma cells. *Med Pediatr Oncol.* 2001;36:104–107.
38. Laiho M, DeCaprio JA, Ludlow JW, et al. Growth inhibition by TGF-beta linked to suppression of retinoblastoma protein phosphorylation. *Cell.* 1990;62:175–185.
39. Reed JC, Meister L, Tanaka S, et al. Differential expression of bcl2 protoonco-

gene in neuroblastoma and other human tumor cell lines of neural origin. *Cancer Res.* 1991;51:6529–6538.

40. Wagner N, Wagner KD, Schley G, et al. The Wilms' tumor suppressor Wt1 is associated with the differentiation of retinoblastoma cells. *Cell Growth Differ.* 2002;13:297–305.
41. Redies C, Takeichi M. N- and R-cadherin expression in the optic nerve of the chicken embryo. *Glia.* 1993;8(3):161–171.
42. Satoh J, Kuroda Y. Beta-catenin expression in human neural cell lines following exposure to cytokines and growth factors. *Neuropathology.* 2000;20: 113–123.
43. Lee MW, Park SC, Chae HS, et al. The protective role of HSP90 against 3-hydroxykynurenine-induced neuronal apoptosis. *Biochem Biophys Res Commun.* 2001;284:261–267.
44. Greenwood JA, Scott CW, Spreen RC, et al. Casein kinase II preferentially phosphorylates human tau isoforms containing an amino-terminal insert. Identification of threonine 39 as the primary phosphate acceptor. *J Biol Chem.* 1994;269:4373–4380.
45. Avila J, Ulloa L, Gonzalez J, et al. Phosphorylation of microtubule-associated proteins by protein kinase CK2 in neuritogenesis. *Cell Mol Biol Res.* 1994;405: 573–579.
46. Ferrari N, Pfahl M, Levi G. Retinoic acid receptor $_{\gamma 1}$ ($RAR_{\gamma 1}$) levels control $RAR_{\beta 2}$ expression in SK-N-BE2(c) neuroblastoma cells and regulate a differentiation-apoptosis switch. *Mol Cell Biol.* 1998;18:6482–6492.

Bone Marrow Transplantation (2004) 33, 255–256

www.nature.com/bmt

Correspondence

Urgent need for a validated tumor response evaluation system for use in immunotherapy

Bone Marrow Transplantation (2004) **33**, 255–256.
doi:10.1038/sj.bmt.1704371
Published online 15 December 2003

Hentschke *et al* recently reported a detailed case series on reduced-intensity stem-cell transplantation (RIST) for the treatment of renal cell and colon cancers.[1] While they provided important information on the feasibility of RIST and its possible antitumor effect, we would like to comment on their study design, especially focusing on the feasibility of response evaluation criteria. Although the Response Evaluation Criteria in Solid Tumors (RECIST) system has been used as a gold standard to evaluate the response of solid tumors to treatment,[2] mainly in the field of cancer chemotherapy, it has not been fully validated in the area of allogeneic transplantation for solid tumors, where the immune-mediated destruction of tumor cells is the principle mechanism of tumor destruction (graft-versus-tumor effect, GVT). Compared to hematological malignancies, solid tumors are generally more resistant to the cytotoxic agents used in conditioning regimens administered before transplantation. Consequently, we considered that there may be some important differences in evaluating the response of solid tumors between RIST and conventional chemotherapy.

First, the feasibility of directly applying RECIST, including the optimal timing of response evaluation, should be critically validated before its extensive application in transplantation. Currently available reports on RIST for solid tumors commonly note that tumor regression occurs several months after transplantation.[3] Some responses and GVHD effects, in general, occur during the late period of RIST. Thus, most tumors continue their natural growth until the manifestation of effective alloimmunity to restrain tumor growth. If the original RECIST criteria[2] are applied to patients undergoing RIST for solid tumors, most of the GVT effects would be evaluated as progressive disease (PD), which would preclude subsequent evaluation (Figure 1a). Therefore, RECIST may underestimate the efficacy of RIST. Furthermore, while there is no concept of spontaneous regression in the field of chemotherapy, this is quite common in RIST.

Second, the proper time to measure the tumor size as a baseline for evaluating a subsequent tumor response has not been clearly defined. In contrast to the results with chemotherapy, the tumor often temporarily increases in size following RIST. Some metastases initially progress slowly, while others progress rapidly. Accordingly, when the size at transplantation is used as a baseline, as in chemotherapy, a therapeutic effect following the initial progression could be overlooked or underestimated (Figure 1c). On the other hand, evaluating regression from the largest size after transplant certainly overestimates the effect of treatment (Figure 1b), and gives an unacceptable bias.

Third, the tumor size after RIST often fluctuates in response to a *de novo* GVT effect, post transplant immunotherapy including donor lymphocyte infusion, and adjustment of immunosuppressive agents (Figure 2). In this situation, it is clear that any evaluation of the response duration, such as progression-free survival and the overall response duration, is essentially impossible using the current RECIST criteria.

These limitations in tumor response evaluation are also expected to be present in other areas including tumor vaccination and dendritic cell therapy strategy. Improved overall survival will ultimately be evaluated in phase III trials. To reach this point, a global standard evaluation system that enables the effective screening of a therapeutic effect in an earlier phase II study will need to be established. We hope that this letter will inspire a productive discussion.

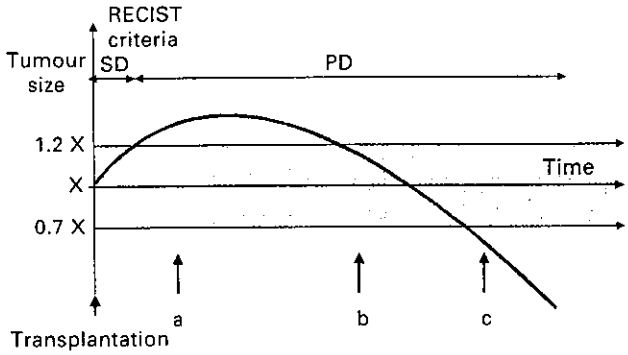

Figure 1 Course of tumor size after transplantation. Primary solid tumors are progressive, despite chemoradiotherapy prior to transplantation. (a) Most tumors continue their natural growth until the development of a GVT effect, which usually occurs several months after transplantation. (b) If the tumor has increased in size compared to that at the time of transplant, regression from the largest size may overestimate the treatment effect. (c) If the tumor size at transplant is defined as a baseline, some treatment effects, observed in patients whose lesions show initial progression followed by regression with the development of GVHD, will be underestimated.

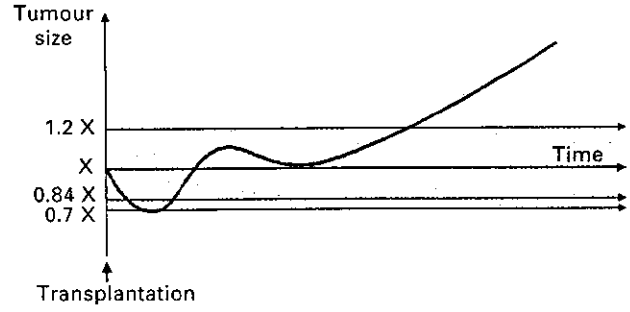

Figure 2 Fluctuation of tumor size after donor lymphocyte infusion or adjustment of immunosuppressive agents. It is difficult to handle patients in whom the tumor size fluctuates in response to post transplant immunotherapy, such as donor lymphocyte infusion and adjustment of immunosuppressive agents. Neither an appropriate timing of response evaluation nor an appropriate time to measure a baseline tumor size has been established in these cases.

A Hori[1]
M Kami[1]
S-W Kim[1]
N Murashige[1]
M Sakiyama[1]
R Kojima[1]
T Hamaki[1]
A Makimoto[1]
S Miyakoshi[2]
S Masuo[3]
S Taniguchi[2]
H Kunitoh[4]
Y Takaue[1]

[1]*Hematopoietic Stem Cell Transplant Unit, National Cancer Center Hospital, 5-1-1, Tsukiji, Chuo-ku, Tokyo 100-0045, Japan;* [2]*Department of Hematology, Toranomon Hospital, Tokyo, Japan;* [3]*Department of Hematology and Rheumatology, JR Tokyo General Hospital, Tokyo, Japan; and* [4]*Department of Internal Medicine and Thoracic Oncology, National Cancer Center Hospital, Tokyo, Japan*

References

1 Hentschke P, Barkholt L, Uzunel M *et al.* Low-intensity conditioning and hematopoietic stem cell transplantation in patients with renal and colon carcinoma. *Bone Marrow Transplant* 2003; **31**: 253–261.

2 Therasse P, Arbuck SG, Eisenhauer EA *et al.* New guidelines to evaluate the response to treatment in solid tumors. European Organization for Research and Treatment of Cancer, National Cancer Institute of the United States, National Cancer Institute of Canada. *J Natl Cancer Inst* 2000; **92**: 205–216.

3 Childs R, Chernoff A, Contentin N *et al.* Regression of metastatic renal-cell carcinoma after nonmyeloablative allogeneic peripheral-blood stem-cell transplantation. *N Engl J Med* 2000; **343**: 750–758.

Journal of Computer Assisted Tomography
27(3):321–326

Adult Neuroblastoma: Radiologic and Clinicopathologic Features

Ukihide Tateishi, Tadashi Hasegawa, Atsushi Makimoto, and Noriyuki Moriyama

Purpose: The purpose of the current study was to define the imaging findings of adult neuroblastoma (ANB) and correlate them with clinicopathologic features.

Materials and Methods: The CT scans and MR images of six patients with histologically confirmed ANB (mean age, 49 years) were retrospectively analyzed.

Results: The arising sites of tumors included the retroperitoneum (n = 2), pelvis (n = 2), anterior mediastinum (n = 1), and adrenal gland (n = 1). The common CT finding was poorly marginated and heterogeneous mass without calcification. Cystic components were often found. On contrast-enhanced CT or MR images, tumors showed heterogeneous enhancement. On T2-weighted images, all masses demonstrated predominantly hyper signal intensity relative to skeletal muscle and the images showed heterogeneous appearance with focal areas of high intensity interspersed with septations of low signal intensity. Soft tissue masses with bone involvement were identified in one case on MR images. The CT findings in one tumor originating from mediastinum were similar to those of tumors arising from other sites.

Conclusion: ANB is an uncommon malignancy that often pursues an aggressive clinical course, involves multiple sites, and has a poor prognosis. Tumors usually manifest on CT or MR images as a poorly demarcated mass mainly in the retroperitoneum and pelvis. Imaging studies can depict aggressive characteristics and disease extent of ANB.

Index Terms: adult neuroblastoma, CT, MRI.

Neuroblastoma is the second most common solid extracranial neoplasm of infancy and childhood. Although more than 90% of cases of this tumor occur in patients younger than 10 years, it has been very occasionally reported in adults. The locations of primary neuroblastomas in adults are similar to the locations in younger patients, with the abdomen and pelvis being the most common areas of occurrence, followed by thorax, head or neck, and extremities.[1] Because of the rarity of adult neuroblastoma (ANB), little is known about its imaging findings and clinicopathologic features.[2–4] In this investigation, we retrospectively reviewed imaging studies of seven cases of ANB to identify the clinicopathologic features, and correlate them.

From the Division of Diagnostic Radiology (U. Tateishi, N. Moriyama), Pathology (T. Hasegaw), and Pediatric Oncology (A. Makimoto), National Cancer Center Hospital and Research Institute, Tokyo, Japan. Address correspondence and reprint requests to Dr. Ukihide Tateishi, Division of Diagnostic Radiology, National Cancer Center Hospital, 5-1-1, Tsukiji, Chuo-Ku, Tokyo, 104-0045, Japan. E-mail: utateish@ncc.go.jp

This work was supported in part by grants for Scientific Research Expenses for Health and Welfare Programs, The Foundation for the Promotion of Cancer Research, and the Second-Term Comprehensive 10-Year Strategy for Cancer Control.

MATERIALS AND METHODS

Medical records and CT and MR images of six patients with ANB were analyzed. Records of all 10 patients who received a diagnosis of ANB from 1990 to 2001 were retrieved from the division of pathology database at our institution. Diagnosis of ANB was based on histologic examination of surgical specimens from affected sites. Of the 10 patients with ANB, 7 had imaging studies available for review. Clinical data and follow-up information were obtained from the referring clinicians and pathologists. The study group comprised three men and three women, ranging in the age from 24 to 74 years (mean 49 years). All patients had prior CT scans (n = 6) or MR examinations (n = 3) that were analyzed retrospectively. Unenhanced and enhanced CT images were obtained in all patients with the use of intravenous iodinated contrast material. Regarding the contrast-enhanced examinations, three patients underwent imaging both in the arterial phase: scan delay set at 30 s after IV contrast administration and delayed phase: scan delay set at 60–80 s, and three underwent only delayed enhanced imaging. MR imaging was performed on one of two models of 1.5-T systems. By using the spin-echo technique, T1-weighted images (repetition time ms/echo time ms, 165–661/4.5–12) were obtained in one or more

planes with (n = 1) or without (n = 2) fat suppression. T2-weighted fast spin echo images (4,500–4,900/112–117) with flow compensation and presaturation superiorly and inferiorly were then obtained in one or more planes using the body coil. The images were obtained with a field of view of 30–40 cm, an image matrix of 128 × 256, and a slice thickness of 10 mm. Gadopentetate dimeglumine was administered IV, and T1-weighted spin echo images were obtained in one or more planes with (n = 1) or without (n = 2) fat suppression. Two radiologists reviewed the CT and MR images, and the findings were reported as a consensus opinion. Locations were judged by type of margin, the extent of tissue involvement, internal architecture, presence of invasion to surrounding tissue, size, signal characteristics on T1- and T2-weighted images, and homogeneity. Signal characteristics were described as isointense or hyperintense relative to the surrounding structures. Pathologic diagnosis was confirmed again by an experienced pathologist. In all cases, tissue slide preparation methods included hematoxylin and eosin, various types of immunohistochemical staining, and molecular analysis by reverse transcription–polymerase chain reaction to differentiate from a primitive neuroectodermal tumor/Ewing's sarcoma.

RESULTS

Clinical Findings

The arising sites of tumors were the retroperitoneum (n = 2), pelvis (n = 2), anterior mediastinum (n = 1), and adrenal gland (n = 1). Presenting symptoms were stated in five patients; the most common symptom was pain in three patients (60%), followed by fever in two, generalized fatigue in one, weight loss in one, pancytopenia in one, and constipation in one. One asymptomatic patient underwent chest CT for the evaluation of anterior mediastinal masses detected on chest radiograph. In four patients whose laboratory data were available, serum levels of both lactic acid dehydrogenase (LDH) and neuron-specific enolase were elevated at the initial examination. On application of the Evans staging criteria for neuroblastoma in all patients, four had stage IV disease and two had stage I disease.[5] Information regarding treatment was available in all patients. Treatment consisted of excision combined with radiation therapy plus chemotherapy (n = 3), excision with chemotherapy (n = 1), and excision alone (n = 2). The most commonly used chemotherapeutic agents were vincristine, cyclophosphamide, doxorubicin HCl (Adriamycin), and cisplatin. Follow-up information on all patients was available. Metastases occurred in four patients. The most frequent sites of metastases were bone (n = 3), followed by liver (n = 2), lymph nodes (n = 2), and other sites, such as soft tissues (n = 1), breast (n = 1), and pleura (n = 1). Three patients with follow-up were dead of disease at a median interval of 3 months (range 1–12 months); two patients were alive with disease at a median interval of 19 months. One patient died of other causes 16 months after the initial treatment.

Imaging Findings and Pathologic Correlation

The lesions ranged from 4.5 to 10.0 cm in maximum dimension, and the median diameter was 7.3 cm. Six lesions were poorly marginated; of these, five were irregular and one was slightly lobulated. No tumor exerted a mass effect upon adjacent structures and crossed the midline to invade the opposite side on both CT and MR imaging. Encasement, displacement, and obstruction of great vessels by primary or metastatic tumor were not found in any cases. Two retroperitoneal masses showed invasive tumor extension in the normal adrenal gland on both CT and MR imaging. On unenhanced CT (n = 6), all lesions were heterogeneous and none of the lesions contained calcification (Fig. 1). Cystic components were identified in four patients; one of these lesions was unilocular and the others were multilocular or multiple (Fig. 1). On contrast-enhanced CT images (n = 6), tumors showed heterogeneous enhancement (Fig. 1). Two lesions demonstrated diffuse enhancement in the arterial phase and decreased enhancement in the delayed phase. One lesion showed punctate enhancement in the arterial phase (Fig. 2). On T1-weighted images, all masses were of low to iso signal intensity compared with that of skeletal muscle. On T2-weighted images, all masses demonstrated predominantly hyper signal intensity relative to skeletal muscle and the images often showed heterogeneous appearance with focal areas of high intensity interspersed with septations of low signal intensity. The pattern of enhancement was heterogeneous on contrast-enhanced MR images (Figs. 1 and 3). Soft tissue masses with bone involvement were identified in one case on MR images (Fig. 3). One tumor of our cases originated from the anterior mediastinum; however, CT findings were similar to those of tumors arising from other sites (Fig. 4).

The solid components of tumors consisted of tumor cells in a trabecular arrangement with multiple lobulation and diffuse vascular proliferation on macroscopic observation. One tumor, which demonstrated punctate enhancement in arterial imaging on contrast-enhanced CT, contained marked dilated vessels within the stromal layer (Fig. 2). Some of the cystic components were admixed with hemorrhage or hemorrhagic necrosis (Fig. 4). Cyst walls were thick and fibrous and encompassed the entire perimeter of the cyst. Lymphatic invasion was seen in three cases; of these, regional lymph node enlargement was seen in two cases both on CT and MR imaging (Fig. 2).

Histologically, all tumors were composed of sheets of small, round cells with hyperchromatic irregular nuclei and scanty cytoplasm that were divided into small lobules by delicate fibrovascular stroma (Fig. 1). There was no calcification in any tumor. Four tumors were subclassified into the undifferentiated subtype and two into the

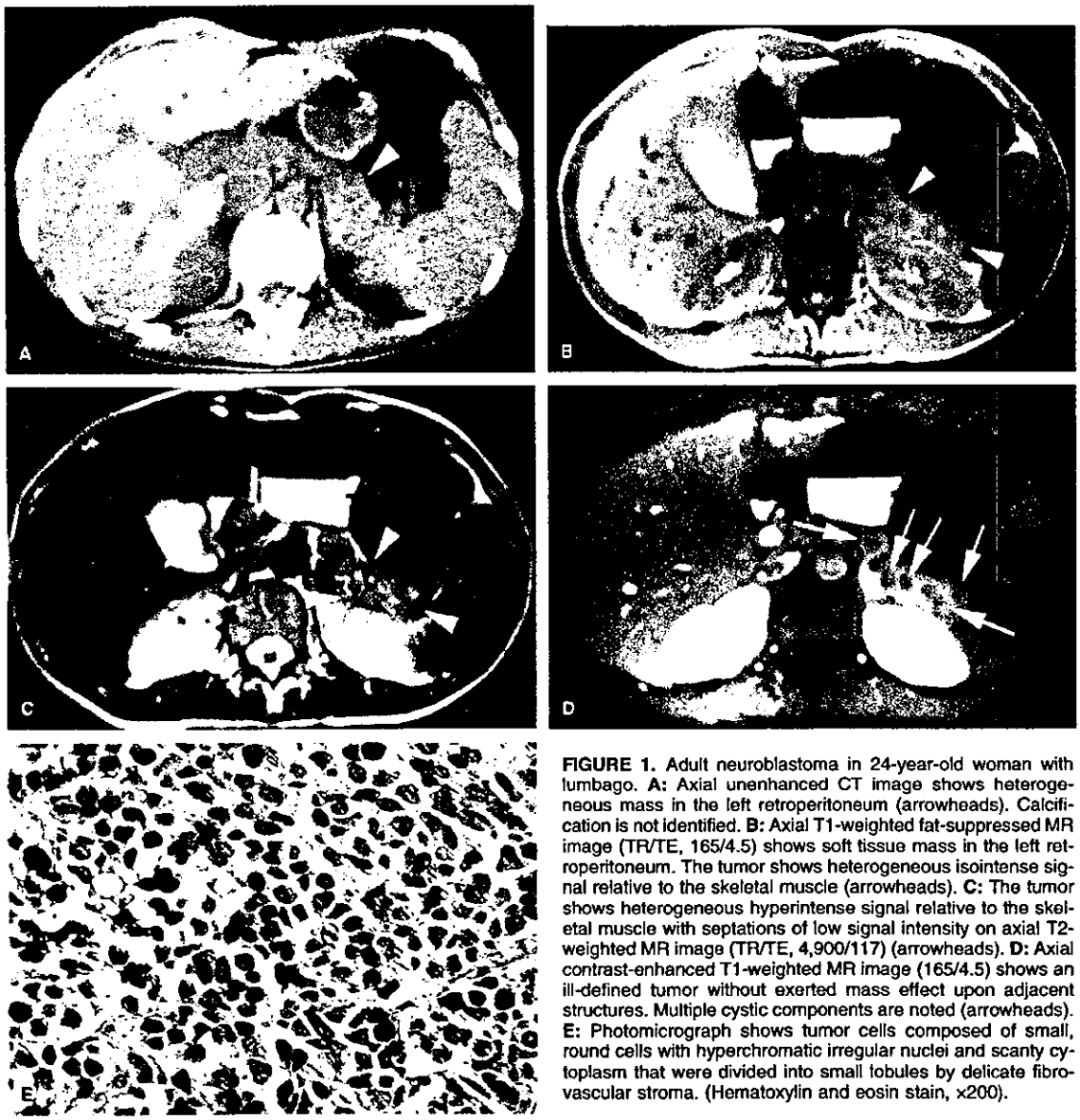

FIGURE 1. Adult neuroblastoma in 24-year-old woman with lumbago. **A:** Axial unenhanced CT image shows heterogeneous mass in the left retroperitoneum (arrowheads). Calcification is not identified. **B:** Axial T1-weighted fat-suppressed MR image (TR/TE, 165/4.5) shows soft tissue mass in the left retroperitoneum. The tumor shows heterogeneous isointense signal relative to the skeletal muscle (arrowheads). **C:** The tumor shows heterogeneous hyperintense signal relative to the skeletal muscle with septations of low signal intensity on axial T2-weighted MR image (TR/TE, 4,900/117) (arrowheads). **D:** Axial contrast-enhanced T1-weighted MR image (165/4.5) shows an ill-defined tumor without exerted mass effect upon adjacent structures. Multiple cystic components are noted (arrowheads). **E:** Photomicrograph shows tumor cells composed of small, round cells with hyperchromatic irregular nuclei and scanty cytoplasm that were divided into small lobules by delicate fibrovascular stroma. (Hematoxylin and eosin stain, ×200).

poorly differentiated subtype according to the Shimada's Classification System.[6,7] Four tumors of poorly differentiated ANB contained abortive pseudorosettes and neuropils. The poorly differentiated tumors were characterized by the development of nuclear enlargement; however, this type did not show differentiation towards ganglion cells. All tumors showed varied immunoreactivity for vimentin and often showed immunoreactivity for multiple neural markers, such as CD56, chromogranin A, synaptophysin, neurofilament, and neuron-specific enolase but were consistently negative for CD99 (O-13). Reverse transcription–polymerase chain reaction analysis on tumor tissues for fusion genes specific for primitive neuroectodermal tumor/Ewing's sarcoma revealed no transcript in all cases, and this evidence was consistent with neuroblastoma.

DISCUSSION

ANB is a rare tumor and a poorly recognized entity that can arise in many sites but most commonly occurs in the retroperitoneum, pelvis, adrenal gland, and mediastinum.[1] Less common sites of origin include the extremities and the neck.[1,8,9] According to the literature, ANB is a tumor that most commonly affects young

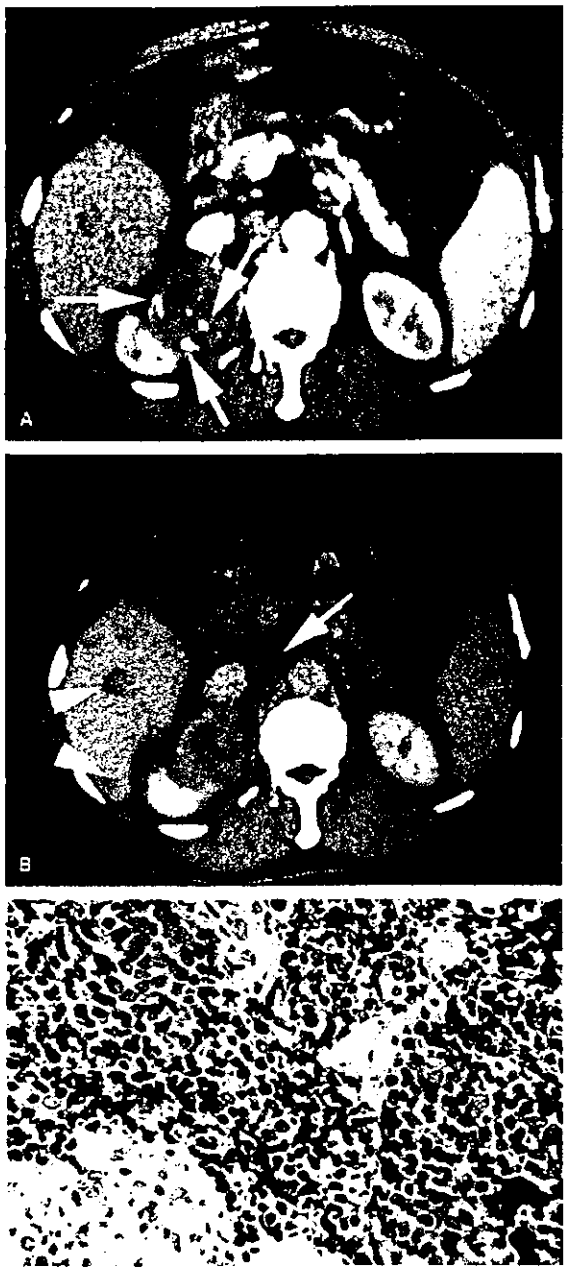

FIGURE 2. Adult neuroblastoma in 56-year-old man with abdominal pain and fever. **A:** Axial enhanced CT image shows poorly marginated tumor in the right adrenal gland. Punctate enhancement (arrows) was seen within the tumor in the arterial phase. **B:** Axial enhanced CT image shows heterogeneous enhancement in the delayed phase. Note pericaval lymph node enlargement (arrow) and hepatic metastasis (arrowheads). **C:** Photomicrograph shows marked dilated vessels within stromal layer and hemorrhage. (Hematoxylin and eosin stain, x200.)

adults who are symptomatic at presentation.[1] The prognosis of patients with ANB is mainly based on the stage of disease. The majority of our patients with stage IV disease died shortly after diagnosis or discovery of disease; however, three patients with stage I disease had an extended duration of survival. As for patients with neuroblastoma in childhood, those with localized disease have an excellent prognosis.[1]

Grossly, ANB forms a nodular, soft to rubbery, firm, and white to gray–pink tumor with areas of hemorrhage on the cut surface. Microscopically, ANB tumors are composed of small, round cells with hyperchromatic irregular nuclei and scanty cytoplasm. Supplementary techniques such as immunohistochemistry, electron microscopy, cytogenetic studies, or a combination of these are thus usually required to establish the diagnosis.[10,11]

CT and MR imaging findings of ANB have been less frequently described and only a few case series are found.[2–4] Calcification within the tumor identified by CT scans is the distinguishing characteristics of primary or metastatic neuroblastoma in children, as described in the previous studies that found an incidence of 50%–80%.[12–16] Calcification exists predominantly in areas of necrosis. Diagnosis of neuroblastoma is sometimes suggested by the presence of calcification existing predominantly in areas of necrosis on microscopic observation.[12] Although some of the cystic components within the

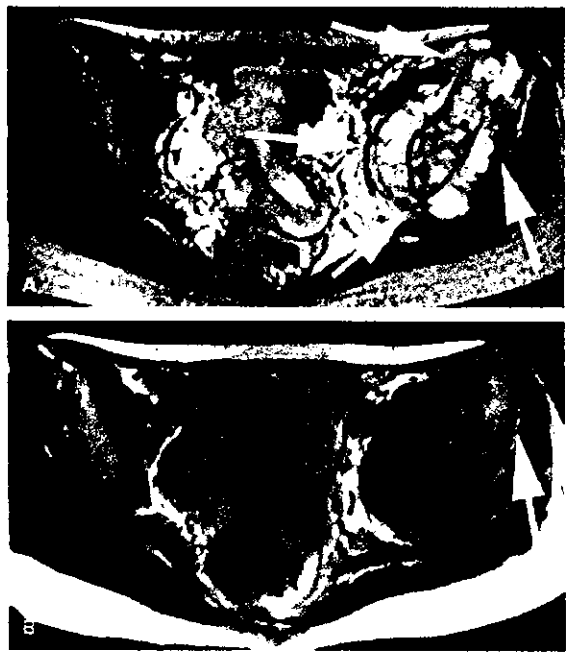

FIGURE 3. Adult neuroblastoma in 30-year-old woman with pain and fever. **A:** Axial T2-weighted MR image (4,500/112) shows poorly marginated tumor (arrows) with predominantly hyper signal intensity relative to skeletal muscle in pelvic wall. **B:** Axial contrast-enhanced T1-weighted MR image (550/12) shows heterogeneous enhancement (arrow) and diffuse involvement of the left iliac bone.

FIGURE 4. Adult neuroblastoma in 72-year-old woman. **A:** Axial enhanced CT image shows poorly marginated tumor in the anterior mediastinum (arrowheads). Note cystic component in the left side (arrows). **B:** Photograph of histopathologic specimen shows solid components of tumor with slightly lobulated configuration (arrows) and cystic components admixed with hemorrhage or hemorrhagic necrosis.

tumors contained hemorrhagic necrosis, none of our cases was associated with calcification in primary or metastatic sites by retrospective assessment of both unenhanced CT scans and microscopic observation. Unlike the CT findings of neuroblastoma in children, the presence of calcification was not a reliable finding in our cases of ANB by both CT and pathologic evaluation, which was in accordance with previous studies.[12–16]

The encasement, displacement, and ultimate obstruction of great vessels by primary or metastatic tumors were described as characteristic signs of neuroblastoma in children.[17,18] Tumors often cross the midline to invade the opposite perirenal space by direct spread of the tumor along the vascular structures.[19] This configuration may mainly rely on the originating site and size of the tumor. None of our cases originated from the perirenal space, and the medium sizes of these tumors were less than those commonly found in childhood cases. However, the infiltrative nature of neuroblastoma allows it to spread over the perirenal space, which may be a causative of various growth patterns on CT or MR imaging.

Although there have been several reports on CT or MR imaging findings of neuroblastoma, little has been discussed on enhancement patterns. We found that contrast-enhanced CT and MR imaging demonstrated a nonspecific, heterogeneous, but relatively hypervascular nature of tumors. In arterial phase, diffuse enhancement was found in two tumors and punctate enhancement in one. This finding reflected the hypervascularity in accordance with diffuse vascular proliferation and stromal dilated vessels of pathologic specimens. All three tumors that underwent T2-weighted MR imaging also showed a heterogeneous architecture with or without septations of low signal intensity. This appearance suggests compartmentalization and a hemorrhagic nature within the tumor. Areas of low signal intensity on T2-weighted images may reflect fibrous solid portions or hemorrhagic changes.

ANB can arise in the mediastinum but less frequently in the anterior mediastinum.[20–23] One tumor of our cases originated from the anterior mediastinum; CT findings were similar to those of tumors arising from the other sites. The tumor consisted of primitive neuroblasts without gangliocytic differentiation on microscopic observation. As for unusual tumor distribution, the possible histogenesis includes malignant transformation of a mediastinal teratoma, aberrantly located in the sympathetic ganglia, neuroectodermal cells native to the normal thymus, and precursors of thymic differentiated epithelial cells.[21–23] The prognosis of mediastinal neuroblastoma has been reported to be better than for other neuroblastomas; surgical resection was performed but the patient died of unrelated causes.[22,23]

In summary, ANB typically often pursues an aggressive clinical course, involves multiple sites, and has a poor prognosis. ANB usually manifests on CT or MR images as a poorly demarcated mass mainly in the retroperitoneum and pelvis. Imaging findings of ANB were nonspecific and similar to neuroblastomas in children; however, the presence of calcification was not a reliable finding on CT. ANB is rare but should be considered in the differential diagnosis for patients with retroperitoneal and pelvic masses.

REFERENCES

1. Franks LM, Bollen A, Seeger RC, et al. Neuroblastoma in adults and adolescents: an indolent course with poor survival. *Cancer* 1997;15;79:2028–35.
2. Feinstein RS, Gatewood OM, Fishman EK, et al. Computed tomography of adult neuroblastoma. *J Comput Assist Tomogr* 1984; 8:720–6.
3. Custodio CM, Semelka RC, Balci NC, et al. Adrenal neuroblastoma in an adult with tumor thrombus in the inferior vena cava. *J Magn Reson Imaging* 1999;9:621–3.
4. Kawakami M, Koda M, Matsunaga N, et al. Adult-type neuroblastoma originated in retroperitoneum beginning with obstructive jaundice. *Clin Imaging* 2001;25:284–7.

5. Evans AE, D'Angio GJ, Propert K, et al. Prognostic factor in neuroblastoma. *Cancer* 1987;59:1853–9.
6. Shimada H, Ambros IM, Dehner LP, et al. Terminology and morphologic criteria of neuroblastic tumors: recommendations by the International Neuroblastoma Pathology Committee. *Cancer* 1999; 86:349–63.
7. Siegel MJ, Ishwaran H, Fletcher BD, et al. Staging of neuroblastoma at imaging: report of the radiology diagnostic oncology group. *Radiology* 2002;223:168–75.
8. Allan SG, Cornbleet MA, Carmichael J, et al. Adult neuroblastoma: report of three cases and review of the literature. *Cancer* 1986;57:2419–21.
9. Kaye JA, Warhol MJ, Kretschmar C, et al. Neuroblastoma in adults: three case reports and a review of the literature. *Cancer* 1986;58:1149–57.
10. Cowan JM, Dayal Y, Schwaitzberg S, et al. Cytogenetic and immunohistochemical analysis of an adult anaplastic neuroblastoma. *Am J Surg Pathol* 1997;21:957–63.
11. Hasegawa T, Hirose T, Ayala AG, et al. Adult neuroblastoma of the retroperitoneum and abdomen: clinicopathologic distinction from primitive neuroectodermal tumor. *Am J Surg Pathol* 2001; 25:918–24.
12. Stark DD, Moss AA, Brasch RC, et al. Neuroblastoma: diagnostic imaging and staging. *Radiology* 1983;148:101–5.
13. Boechat MI, Ortega J, Hoffman AD, et al. Computed tomography in stage III neuroblastoma. *AJR Am J Roentgenol* 1985;145: 1283–7.
14. Cremin BJ, Mervis B. Paediatric abdominal computed tomography: the technique and use in neuroblastomas and pelvic masses. *Br J Radiol* 1983;56:291–8.
15. Berdon WE, Stylianos S, Ruzal-Shapiro C, et al. Neuroblastoma arising from the organ of Zuckerkandl: an unusual site with a favorable biologic outcome. *Pediatr Radiol* 1999;29:497–502.
16. David R, Lamki N, Fan S, et al. The many faces of neuroblastoma. *Radiographics* 1989;9:859–82.
17. Peretz GS, Lam AH. Distinguishing neuroblastoma from Wilms tumor by computed tomography. *J Comput Assist Tomogr* 1985; 9:889–93.
18. Rosenfield NS, Leonidas JC, Barwick KW. Aggressive neuroblastoma simulating Wilms tumor. *Radiology* 1988;166:165–7.
19. Oliphant M, Berne AS. Mechanism of direct spread of abdominal neuroblastoma: CT demonstration and clinical implications. *Gastrointest Radiol* 1987;12:59–66.
20. Argani P, Erlandson RA, Rosai J. Thymic neuroblastoma in adults: report of three cases with special emphasis on its association with the syndrome of inappropriate secretion of antidiuretic hormone. *Am J Clin Pathol* 1997;108:537–43.
21. Salter JE Jr, Gibson D, Ordonez NG, et al. Neuroblastoma of the anterior mediastinum in an 80-year-old woman. *Ultrastruct Pathol* 1995;19:305–10.
22. Suita S, Tajiri T, Sera Y, et al. The characteristics of mediastinal neuroblastoma. *Eur J Pediatr Surg* 2000;10:353–9.
23. Yamamo R, Tada H, Kishi A, et al. Neuroblastoma resection in an adult with a 10-year history of chest mass shadow. *Jpn J Thorac Cardiovasc Surg* 2000;48:809–11.

Int J Clin Oncol (2004) 9:7–12
DOI 10.1007/s10147-003-0364-2

REVIEW ARTICLE

Atsushi Makimoto

Results of treatment of retinoblastoma that has infiltrated the optic nerve, is recurrent, or has metastasized outside the eyeball

Received: November 6, 2003

Abstract Since the development of chemotherapy regimens for patients with retinoblastoma started in the 1950s, various agents and regimens have been employed for various kinds of patients. Chemotherapy has been employed for: (1) patients with high-risk features for metastases, such as patients with optic nerve involvement, (2) patients with orbital involvement, and (3) patients with distant metastasis. Effective systemic chemotherapeutic agents include vincristine, doxorubicin, cyclophosphamide, etoposide, cisplatin, and carboplatin, and, as well, intrathecal agents, including methotrexate, cytarabine, and corticosteroids are available. With the addition of appropriate chemotherapies to the conventional treatment modalities such as enucleation and radiotherapy, patients with advanced retinoblastoma are expected to obtain a survival benefit. Moreover, a new modality combined with autologous stem cell support allowed us to use high-dose alkylating agents such as thiotepa, melphalan, and cyclophosphamide, which resulted in better prognosis for patients with metastatic retinoblastoma. Because of the small number of patients with retinoblastoma and the diversity of the disease characteristics in individual patients, there have been no clinical trials to determine whether to recommend a particular regimen, or to identify specific criteria in patients who would benefit from chemotherapy. Well-designed prospective controlled trials are warranted to establish a standard treatment strategy for patients with extraocular retinoblastoma.

Key words Retinoblastoma · Adjuvant chemotherapy
High-dose chemotherapy · Stem cell transplantation

A. Makimoto (✉)
Division of Pediatric Oncology, National Cancer Center Hospital, 5-1-1 Tsukiji, Chuo-ku, Tokyo 104-0045, Japan
Tel. +81-3-3542-2511; Fax +81-3-3542-3815
e-mail: amakimot@ncc.go.jp

Introduction

Although primary enucleation in patients with retinoblastoma has produced excellent prognosis,[1] there are several populations in which further treatment is necessary to prevent progression or recurrence.[2–8] Such high-risk populations include: (1) patients with optic nerve involvement, (2) patients with orbital involvement, (3) patients with distant metastasis, (4) patients with central nervous system (CNS) involvement, and (5) patients with trilateral retinoblastoma. Although treatment strategies for each population could differ, multiagent chemotherapy has been the main modality used in postoperative treatments. For some patients with extensive disease, such as distant metastasis or CNS involvement, intensive chemotherapy with autologous hematopoietic stem cell transplantation (SCT) may be indicated. In this article, a review of data in the literature and the results of our retrospective analyses of case series will be discussed, in order to describe the role of chemotherapy in patients with advanced retinoblastoma.

Overview of the development of chemotherapy regimens for patients with retinoblastoma

The development of chemotherapy regimens for patients with retinoblastoma started in the 1950s.[9–11] Through the accumulation of data in several case series including patients with metastatic disease, the efficacy of vincristine, cyclophosphamide, and doxorubicin was established by the 1980s.[12,13] After the 1980s, combinations of etoposide and cisplatin or carboplatin were developed through trials that mainly recruited patients with retinoblastoma with orbital extension.[14,15] These chemotherapy regimens are currently being employed for patients with early-stage retinoblastoma in attempts to preserve the eye.[16] Although the issue of neoadjuvant chemoreduction therapy and eye preservation is one of the most controversial issues in the treatment of retinoblastoma, it will be discussed in another article, by

Tosiaki Yanagisawa, in this issue of the International Journal of Clinical Oncology (pages 13–24).

Adjuvant chemotherapy for patients with optic nerve involvement

Considering the fact that the majority of patients with retinoblastoma can be cured by primary enucleation, with or without adjuvant chemoradiotherapy, the selection of patients who have a high risk of metastasis is important. Several risk factors that could predict eventual metastasis in patients with retinoblastoma after enucleation have been suggested in several retrospective studies.[2–8] The risk factors suggested to date have been patients with: (1) extensive choroidal involvement, (2) disease extending to the sclera, (3) intraorbital disease, (4) ciliary body or iris involvement, or (5) disease extending beyond the lamina cribrosa, with or without involvement of the cut end of the optic nerve.

According to data reported by Shields et al.,[6,7] 67 (23 %) of 289 patients with retinoblastoma had histopathological evidence of choroidal invasion. Although these patients were more likely to develop metastases than those without choroidal invasion ($P = 0.0001$), isolated choroidal invasion alone was not a significant risk factor ($P = 0.10$). In contrast, 84 (29%) of the same 289 patients had optic nerve invasion; with prelaminar invasion accounting for 15%, laminar, 7%; postlaminar with the cut end of the optic nerve, 6%; and post laminar without the cut end of the optic nerve, 1%. Among these 84 patients, only optic nerve invasion beyond the lamina cribrosa (laminar and postlaminar invasion) was a significant predictor of metastases ($P = 0.0001$). Magramm et al.[4] reported that the mortality rate was as high as 42% in patients with invasion beyond the lamina cribrosa, and 78% in patients with invasion beyond the cut end.

Prophylactic adjuvant chemotherapy in patients with retinoblastoma who have some of the above risk factors probably reduces the risk of metastases and recurrence.[17] Although each institute or group usually stratifies their treatment strategy based on the pathological findings noted above, an appropriate regimen of adjuvant chemotherapy for each disease type has not been conclusively determined.

Zelter et al.[13] used enucleation and chemotherapy that included cyclophosphamide, vincristine, and doxorubicin for tumors involving the optic nerve head, and additional cranial radiation with intrathecal chemotherapy for tumors extending beyond the cut end. Although the number of patients was limited, the overall survival rates were 100% (6 of 6) for patients with optic nerve extension without cut-end disease, 75% (3 of 4) for patients with unilateral disease and cut-end disease, and 50% (1 of 2) for patients with bilateral disease and cut-end disease.

Acquaviva et al.[18] reported a series of 51 patients (32 with unilateral disease and 19 with bilateral disease) who underwent systemic chemotherapy. Patients with disease extending to the optic nerve head, choroid, and emissaries received cyclophosphamide and vincristine in addition to local radiotherapy. Doxorubicin was added when there was invasion beyond the cut end or through the sclera into the orbit. In patients with CNS involvement, intrathecal chemotherapy and cranial radiation were added. The overall survival rate was 90.6% for patients with unilateral disease and 84.2% for patients with bilateral disease.

Schvartzman et al.[19] reported the results of a stage-based treatment strategy in a total of 116 consecutive patients. A total of 25 patients with optic nerve invasion (11 with invasion up to the cut end, and 14 with invasion beyond the cut end) received chemotherapy that included vincristine, doxorubicin, and cyclophosphamide for 57 weeks, and they also received 40–45 Gy of orbital radiotherapy. Intrathecal chemotherapy that included methotrexate, cytarabine, and dexamethasone was added for the patients with evidence of cut-end disease. Twenty-one of the 25 patients had survived at the end of a median follow-up time of 39 months.

These data suggest that patients with optic nerve invasion would benefit from adjuvant chemotherapy and orbital radiotherapy. Orbital radiation could be omitted in patients with tumor extension not reaching the cut end of the optic nerve. The indication for cranial radiation should be reserved for patients with CNS involvement.

Adjuvant chemotherapy for patients with orbital extension

Different from the indications for micrometastatic retinoblastoma discussed above, adjuvant chemotherapy and/or radiotherapy are absolutely necessary when patients have evidence of macroscopic extraocular residual tumor, such as invasion to the orbital space and distant metastases. Patients with orbital extension of retinoblastoma had been associated with a high mortality rate, of close to 100%, before the development of chemotherapy.[11]

Doz et al.[14] treated a total of 33 patients with orbital extension of retinoblastoma with combinations of systemic and intrathecal chemotherapy, and orbital and/or cranial radiotherapy. The overall survival rate was 34%, with a median follow-up of 3.5 years. The same group conducted a phase II study to test the efficacy and safety of a combination chemotherapy comprising etoposide 100 mg/m^2 for 5 days and carboplatin 160 mg/m^2 for 5 days.[15] The response rate for the 20 patients was 85% (17 patients), including 9 complete responders.

Kiratli et al.[20] reported a total of 16 patients with massive orbital involvement of retinoblastoma who received various combinations of therapeutic approaches, including multiagent chemotherapy. Twelve of the 16 patients were alive and disease-free at a median duration of follow-up of 22 months.

These results suggest that patients with orbital extension of retinoblastoma could obtain a survival benefit when chemotherapy is used in combination with appropriate radiation therapy.

Retrospective analysis of patients who received adjuvant chemotherapy at the National Cancer Center Hospital (NCCH), Japan

A total of 59 patients with advanced retinoblastoma received scheduled chemotherapy (described in Table 1) during the period from May 1980 through October 2001 at the NCCH. While 41 patients had optic nerve invasion without distant metastasis, 18 patients had distant metastases. The disease criteria and treatment regimens are described in Table 2. The dose-intensity of chemoradiotherapy was determined according to the degree of tumor extension. The three different chemotherapy regimens listed in Table 1 were mainly employed. Regimen A only was used as the adjuvant chemotherapy regimen until 1990, when etoposide and cisplatin (regimen B) became available in the pediatric field, and the alternating use of regimen A and regimen B started. Regimen C, a chemotherapy regimen used for advanced neuroblastoma, was employed for patients with metastatic disease.[21] Figure 1 shows the overall survival data, stratified by the year-period when the patients started chemotherapy. Although the overall survival rate of the 59 patients was only 70%, there was a significant improvement in the rate in patients treated after 1990. The overall survival rate of patients treated after January 1990 was 89%, while that of patients treated between May 1980 and December 1989 was only 54%.

In a subgroup analysis according to the St. Jude staging system,[22] the stage IV patients who were treated in the 1980s had a shorter duration of overall survival after completion of chemotherapy than the patients with stage II–III disease, although the difference was not statistically significant by the log-rank test (P = 0.07). In contrast, patients treated after 1990 did not have such a tendency; the patients with stage IV disease had a survival period identical to that in patients with stage II–III disease (Fig. 2). In other words, the addition of etoposide and cisplatin contributed to an improvement in survival for the St. Jude stage IV patients, but not for the patients with less advanced disease. According to Cox proportional hazard analysis, three factors: age less than 2 years at the diagnosis, St. Jude stage IV, and treatment before 1990 (regimen A alone) were considered to be major risk factors. Based upon these data, age and clinical stage could be utilized as risk factors to determine the post-enucleation chemotherapy, and regimen A (vincristine, pirarubicin, cyclophosphamide) may be

Table 1. Chemotherapy regimens

Name of regimen	Drugs	Dose (mg/m^2)	Days
Regimen A	Vincristine	1.5	1
	Cyclophosphamide	600–800	2 and 3
	Pirarubicin	40	4
Regimen B	Etoposide	100	1 to 5
	Cisplatin	20	1 to 5
Regimen C	Cyclophosphamide	1200	1
	Pirarubicin	40	3
	Etoposide	100	1 to 5
	Cisplatin	90	5

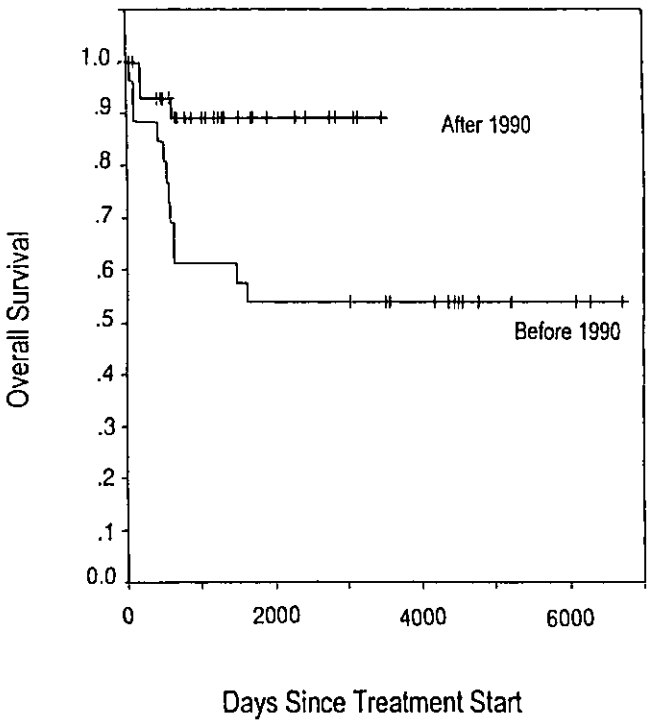

Fig. 1. Overall survival according to the time period of treatment

Table 2. Treatment criteria

Criteria	Degree of disease extension	Chemotherapy	Radiotherapy
1	Infiltration beyond the lamina cribrosa or infiltration to the anterior chamber	Alternating regimen A and regimen B every 8 weeks; a total of 3 cycles	None
2	Invasion into the orbit through the sclera	Alternating regimen A and regimen B every 8 weeks; a total of 3 cycles	40–60 Gy, orbital
3	Massive infiltration to the orbit	Alternating regimen A and regimen B every 6 weeks; a total of 4 cycles	40–60 Gy, orbital
4	Invasion beyond cut end of the optic nerve	Alternating regimen A and regimen B every 6 weeks; a total of 4 cycles; intrathecal chemotherapy every 6 weeks	40–60 Gy, orbital
5	Distant metastases	Regimen C every 4 weeks; a total of 4–6 cycles, followed by HDC	40–60 Gy, local

HDC, high-dose chemotherapy